

Gamma irradiation-induced defects in borosilicate glasses for high-level radioactive waste immobilisation

RAUTIYAL, Prince, GUPTA, Gaurav, EDGE, Ruth, LEAY, Laura, DAUBNEY, Aaron, PATEL, Maulik, JONES, Alan and BINGHAM, Paul
<<http://orcid.org/0000-0001-6017-0798>>

Available from Sheffield Hallam University Research Archive (SHURA) at:

<http://shura.shu.ac.uk/27681/>

This document is the author deposited version. You are advised to consult the publisher's version if you wish to cite from it.

Published version

RAUTIYAL, Prince, GUPTA, Gaurav, EDGE, Ruth, LEAY, Laura, DAUBNEY, Aaron, PATEL, Maulik, JONES, Alan and BINGHAM, Paul (2020). Gamma irradiation-induced defects in borosilicate glasses for high-level radioactive waste immobilisation. *Journal of Nuclear Materials*.

Copyright and re-use policy

See <http://shura.shu.ac.uk/information.html>

Figure S1. XRD patterns for NaBaBSi and LiNaBSi pristine glasses.

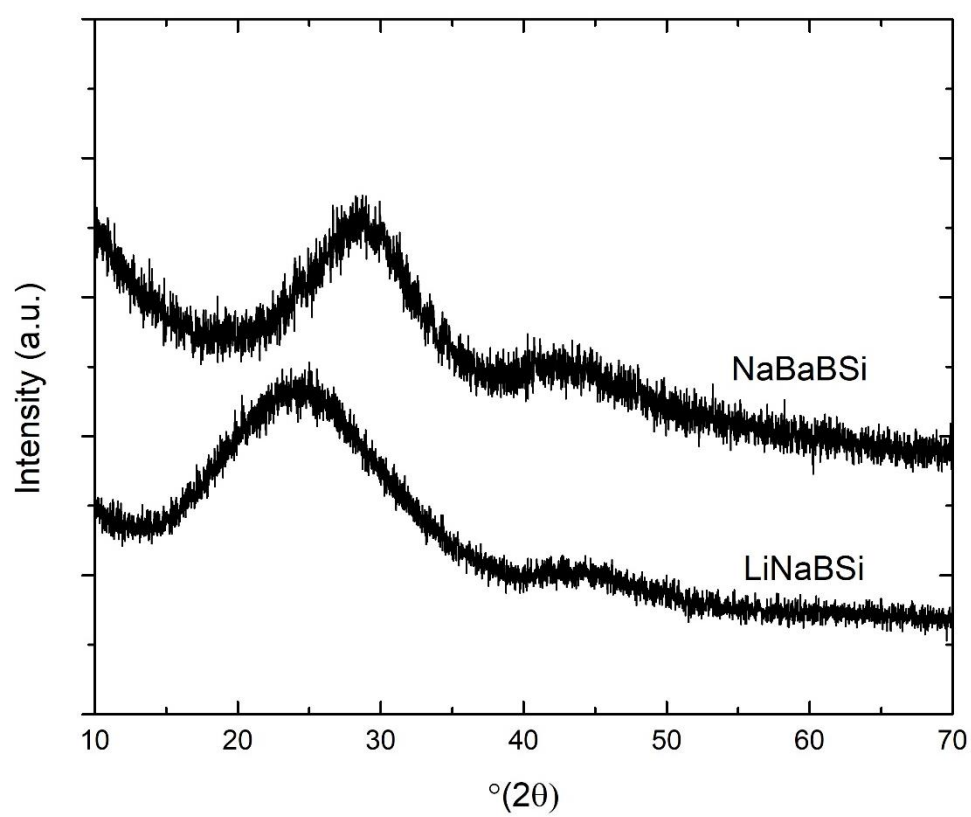


Figure S2. Intensity-normalised first derivative EPR spectra for NaBaBSi glass irradiated with 0.5MGy annealed for 16 hours at different temperatures.

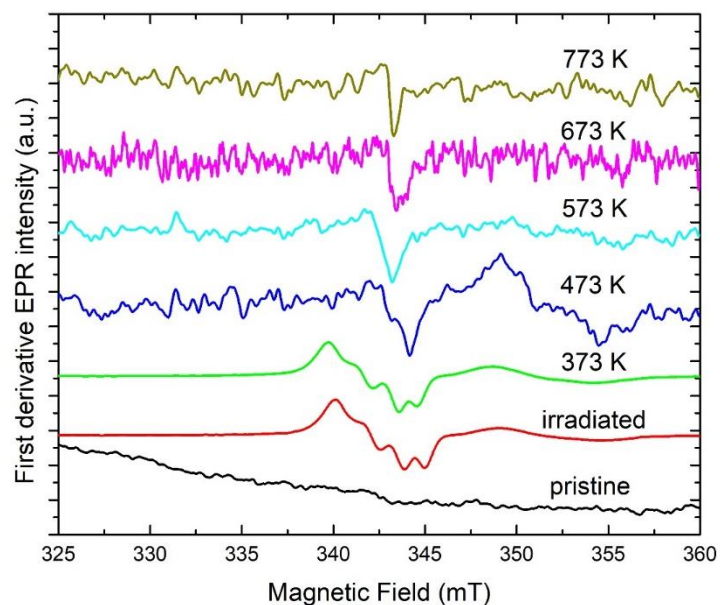


Figure S3. Intensity-normalised second derivative EPR spectra for NaBaBSi glass irradiated with 0.5MGy annealed for 16 hours at different temperatures.

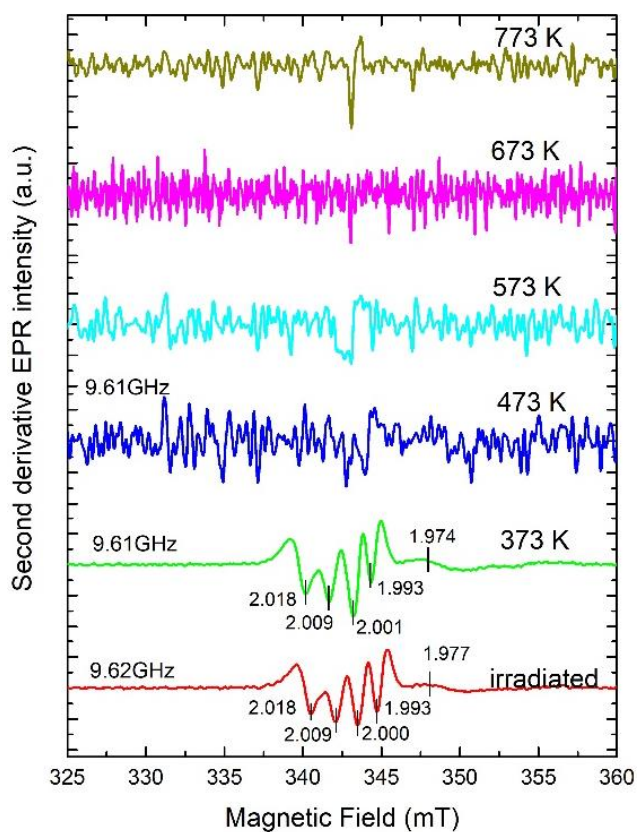


Table S1. The *g*-values and defect types for NaBaBSi glass irradiated with 0.5MGy annealed for 16 hours at different temperatures.

NaBaBSi 0.5 MGy 16 hrs									
373 K		473 K		573 K		673 K		773 K	
<i>g</i> -value	defect	<i>g</i> -value	defect	<i>g</i> -value	defect	<i>g</i> -value	defect	<i>g</i> -value	defect
2.019	BOHC/E ⁻	low S/N	-	low S/N	-	Annihilated/Recombined			
2.009	BOHC	low S/N	-	low S/N	-				
2.001	BOHC	low S/N	-	low S/N	-				
1.993	ET	low S/N	-	low S/N	-				
1.974	E ⁻	low S/N	-	low S/N	-				

*Note: Low S/N ratio means concentration of defects have become very low due to defect recombination/annihilation that the calculation of *g*-value was not possible.*

Figure S4. Intensity-normalised first derivative EPR spectra for NaBaBSi irradiated with 0.5MGy annealed for 24 hours at different temperatures.

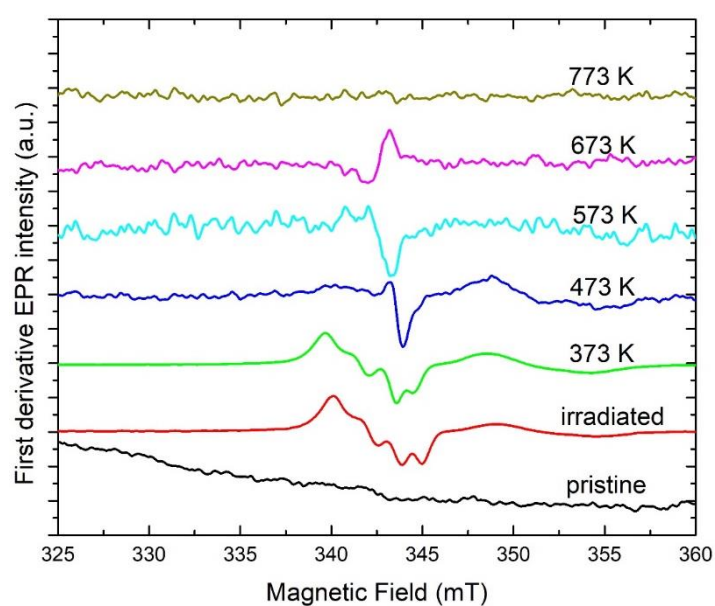


Figure S5. Intensity-normalised second derivative EPR spectra for NaBaBSi irradiated with 0.5MGy annealed for 24 hours at different temperatures.

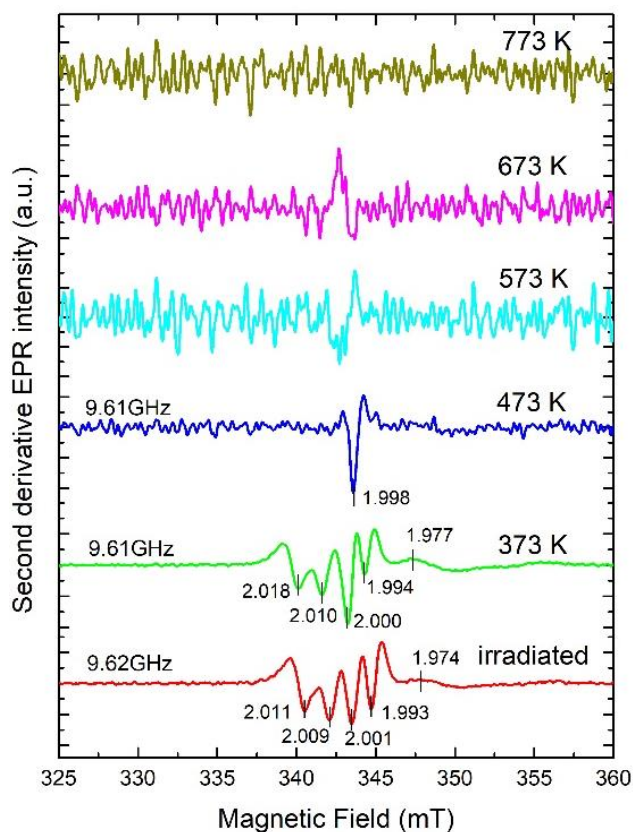


Table S2. The g-values and defect types for NaBaBSi glass irradiated with 0.5MGy annealed for 24 hours at different temperatures.

NaBaBSi 0.5 MGy 24 hrs									
373 K		473 K		573 K		673 K		773 K	
g-value	defect	g-value	defect	g-value	defect	g-value	defect	g-value	defect
2.019	BOHC/E ⁻	1.998	E'	low S/N	-	Annihilated/Recombined			
2.010	BOHC	low S/N	-	low S/N	-				
2.000	BOHC	low S/N	-	low S/N	-				
1.994	ET	low S/N	-	low S/N	-				
1.977	E ⁻	low S/N	-	low S/N	-				

Figure S6. Intensity-normalised first derivative EPR spectra for NaBaBSi irradiated with 5 MGy annealed for 16 hours at different temperatures.

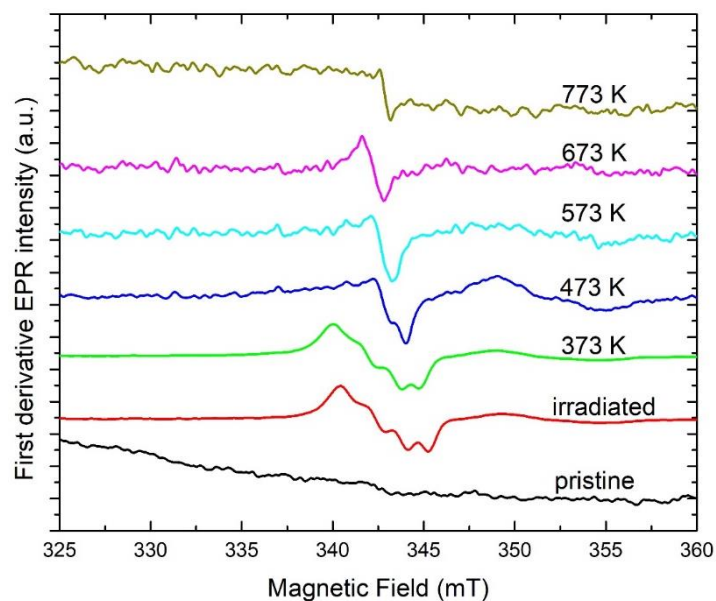


Figure S7. Intensity-normalised second derivative EPR spectra for NaBaBSi glass irradiated with 5 MGy annealed for 16 hours at different temperatures.

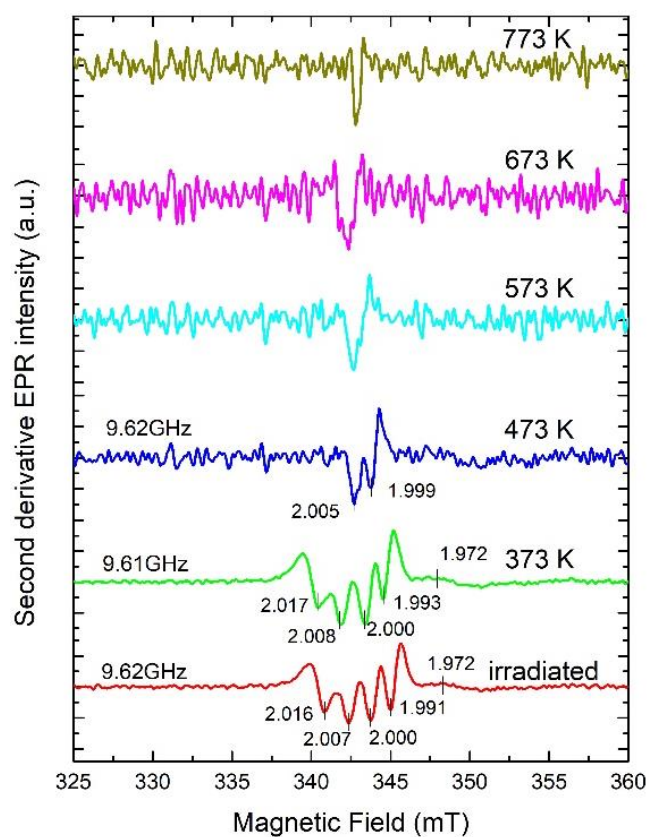


Table S3. The g-values and defect types for NaBaBSi glass irradiated with 5 MGy annealed for 16 hours at different temperatures.

NaBaBSi 5 MGy 16 hrs									
373 K		473 K		573 K		673 K		773 K	
g-value	defect	g-value	defect	g-value	defect	g-value	defect	g-value	defect
2.017	BOHC/E ⁻	2.005	POR	low S/N	-	Annihilated/Recombined			
2.008	BOHC	1.999	POR	low S/N	-				
2.000	BOHC			low S/N	-				
1.993	ET			low S/N	-				
1.972	E ⁻			low S/N	-				

Figure S8. Intensity-normalised first derivative EPR spectra for NaBaBSi irradiated with 5MGy annealed for 24 hours at different temperatures.

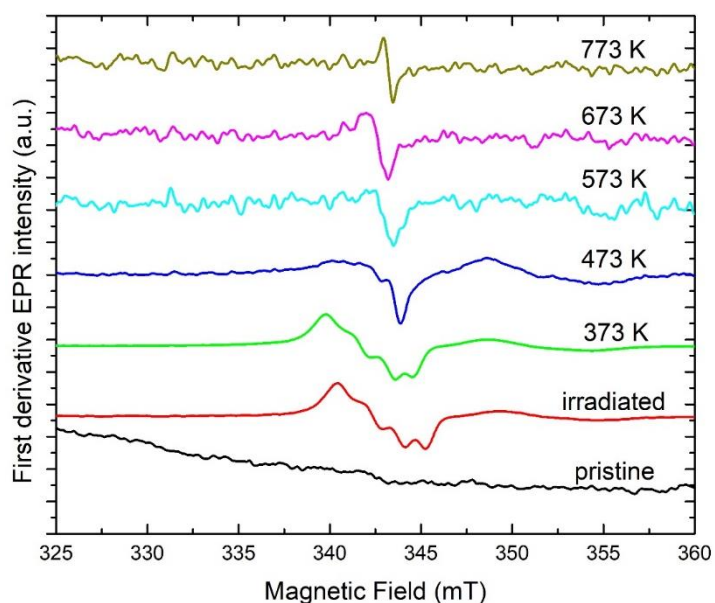


Figure S9. Intensity-normalised second derivative EPR spectra for NaBaBSi irradiated with 5MGy annealed for 24 hours at different temperatures.

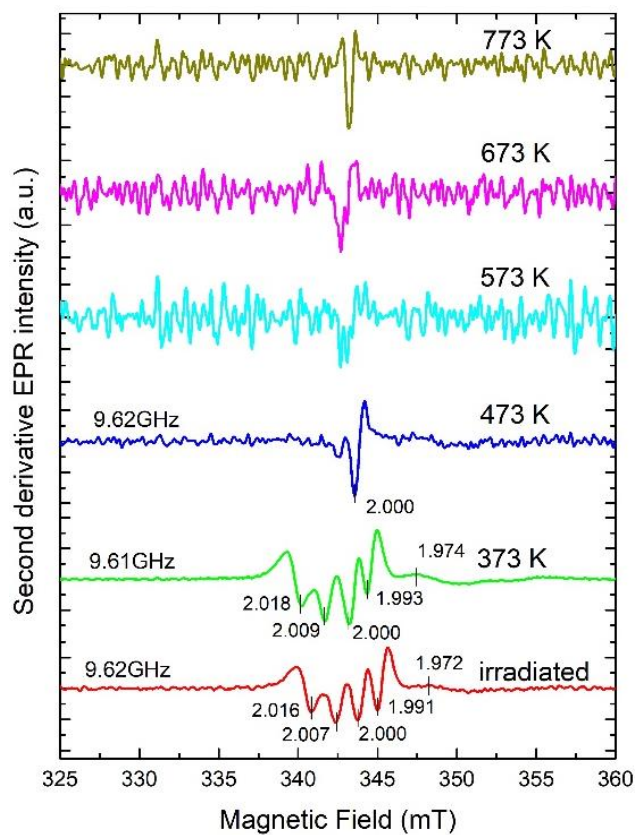


Table S4. The g-values and defect types for NaBaBSi glass irradiated with 5 MGy annealed for 24 hours at different temperatures.

NaBaBSi 5 MGy 24 hrs									
373 K		473 K		573 K		673 K		773 K	
g-value	defect	g-value	defect	g-value	defect	g-value	defect	g-value	defect
2.018	BOHC/E ⁻	2.000	POR	low S/N	-	Annihilated/Recombined			
2.009	BOHC			low S/N	-				
2.000	BOHC			low S/N	-				
1.993	ET			low S/N	-				
1.974	E ⁻			low S/N	-				

Figure S10. Intensity-normalised first derivative EPR spectra for LiNaBSi irradiated with 0.5MGy annealed for 16 hours at different temperatures.

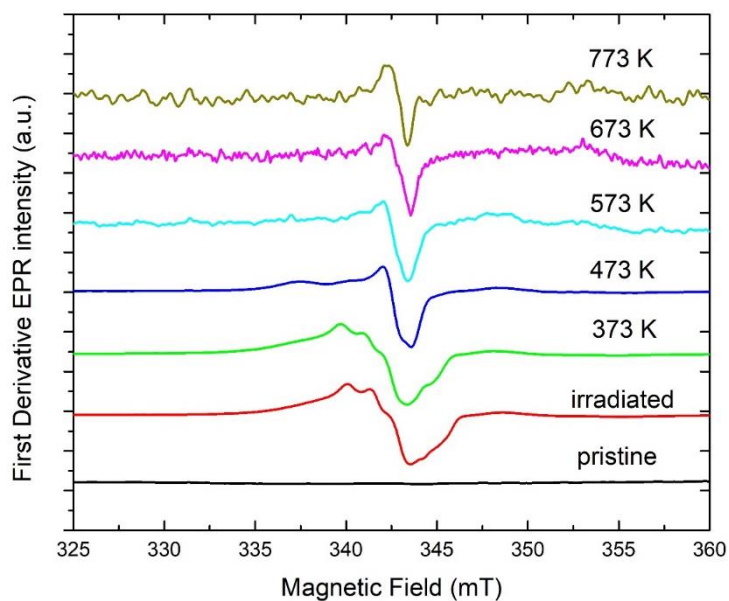


Figure S11. Intensity-normalised second derivative EPR spectra for LiNaBSi irradiated with 0.5MGy annealed for 16 hours at different temperatures.

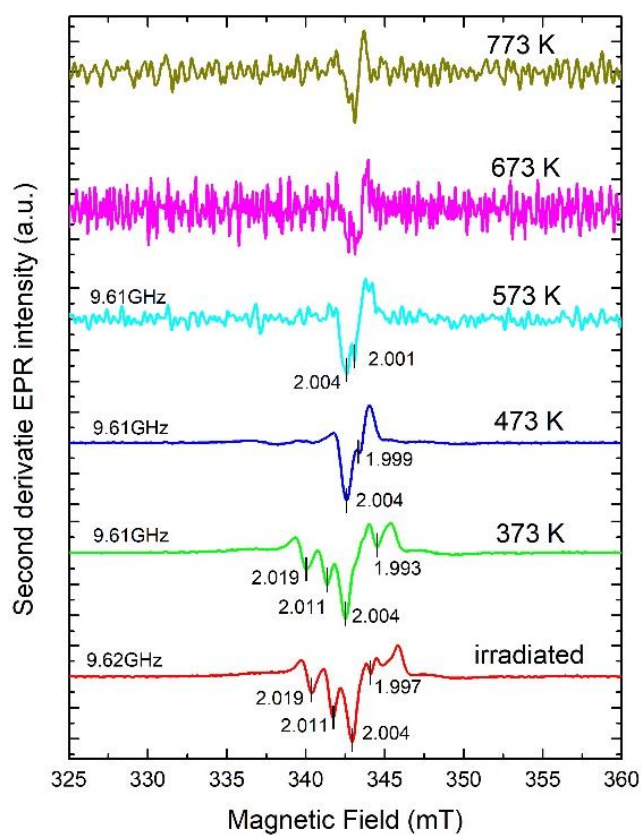


Table S5. The *g*-values and defect types for LiNaBSi glass irradiated with 0.5 MGy annealed for 16 hours at different temperatures.

LiNaBSi 0.5 MGy 16 hrs									
373 K		473 K		573 K		673 K		773 K	
<i>g</i> -value	defect	<i>g</i> -value	defect	<i>g</i> -value	defect	<i>g</i> -value	defect	<i>g</i> -value	defect
2.019	BOHC	2.004	PORs	2.004	POR	Annihilated/Recombined			
2.012	BOHC	1.999	PORs	2.001	POR				
2.005	BOHC	low S/N	-	low S/N	-				
1.993	ET	low S/N	-	low S/N	-				

Figure S12. Intensity-normalised first derivative EPR spectra for LiNaBSi irradiated with 0.5MGy annealed for 24 hours at different temperatures.

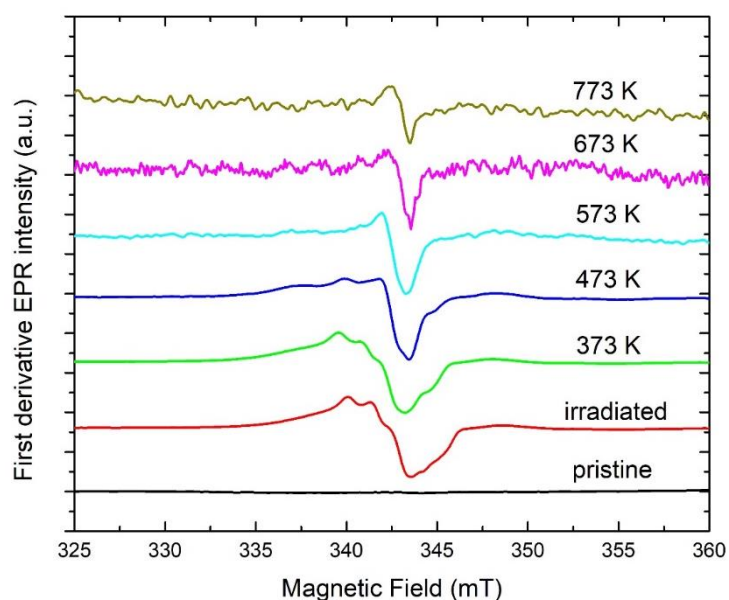


Figure S13. Intensity-normalised second derivative EPR spectra for LiNaBSi irradiated with 0.5MGy annealed for 24 hours at different temperatures.

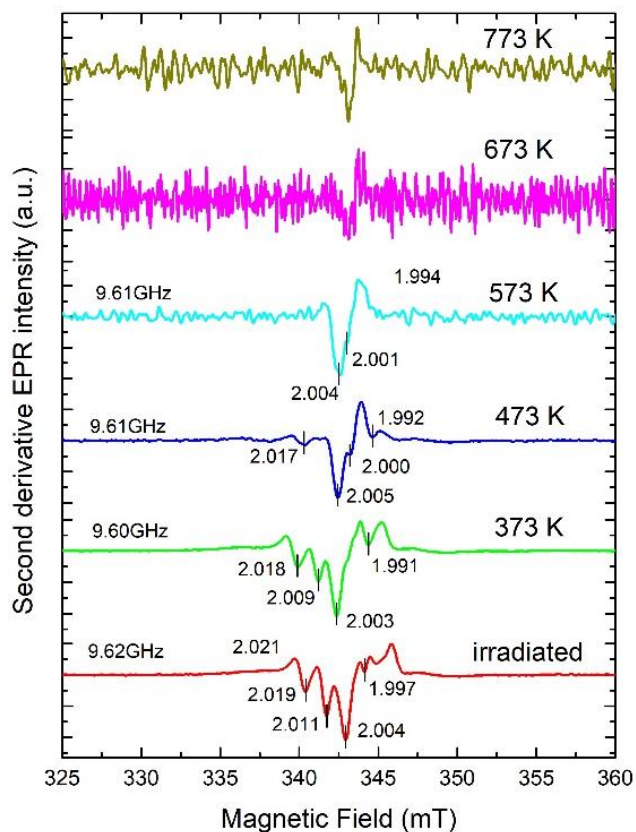


Table S6. The g-values and defect types for LiNaBSi glass irradiated with 0.5 MGy annealed for 24 hours at different temperatures.

LiNaBSi 0.5 MGy 24 hrs									
373 K		473 K		573 K		673 K		773 K	
g-value	defect	g-value	defect	g-value	defect	g-value	defect	g-value	defect
2.018	BOHC	2.017	POR	2.004	POR	Annihilated/Recombined			
2.009	BOHC	2.005	POR	2.001	POR				
2.003	BOHC	2.000	POR	low S/N	-				
1.991	ET	1.992	ET	low S/N	-				

Figure S14. Intensity-normalised first derivative EPR spectra for LiNaBSi irradiated with 5MGy annealed for 16 hours at different temperatures.

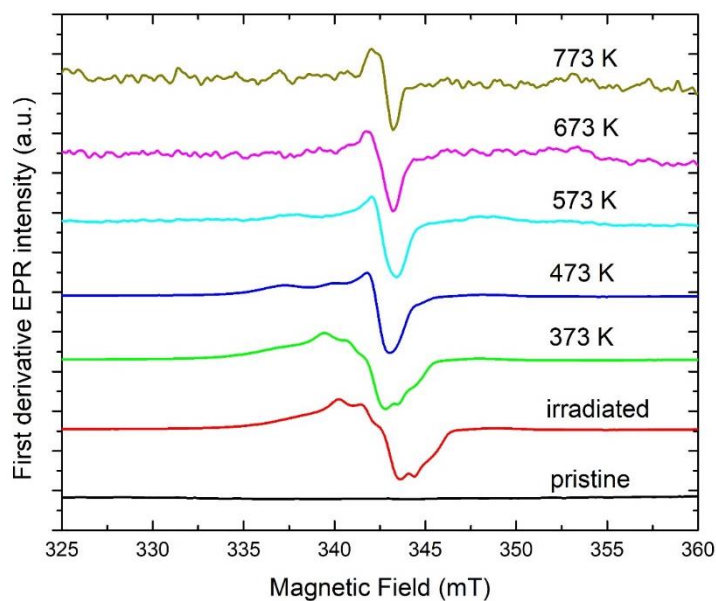


Figure S15. Intensity-normalised second derivative EPR spectra for LiNaBSi irradiated with 5MGy annealed for 16 hours at different temperatures.

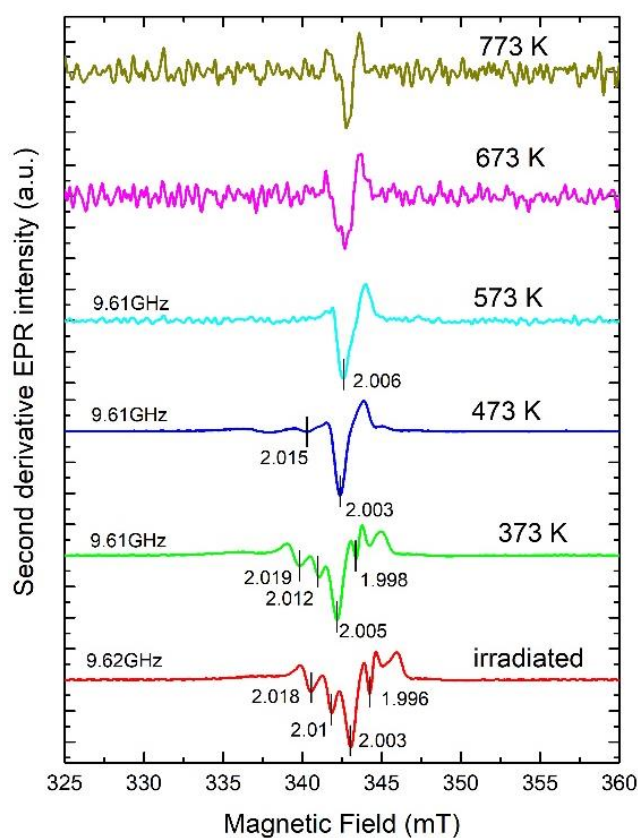


Table S7. The *g*-values and defect types for LiNaBSi glass irradiated with 5 MGy annealed for 16 hours at different temperatures.

LiNaBSi 5 MGy 24 hrs									
373 K		473 K		573 K		673 K		773 K	
<i>g</i> -value	defect	<i>g</i> -value	defect	<i>g</i> -value	defect	<i>g</i> -value	defect	<i>g</i> -value	defect
2.019	BOHC	2.015	POR	2.006	POR	Annihilated/Recombined			
2.012	BOHC	2.003	POR	low S/N	-				
2.005	BOHC	low S/N	-	low S/N	-				
1.998	ET	low S/N	-	low S/N	-				

Figure S16. Intensity-normalised first derivative EPR spectra for LiNaBSi irradiated with 5MGy annealed for 24 hours at different temperatures.

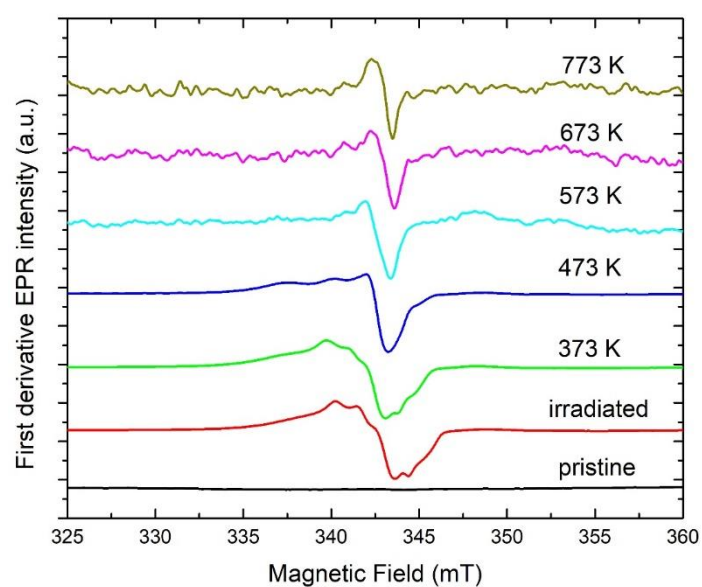


Figure S17. Intensity-normalised second derivative EPR spectra for LiNaBSi irradiated with 5MGy annealed for 24 hours at different temperatures.

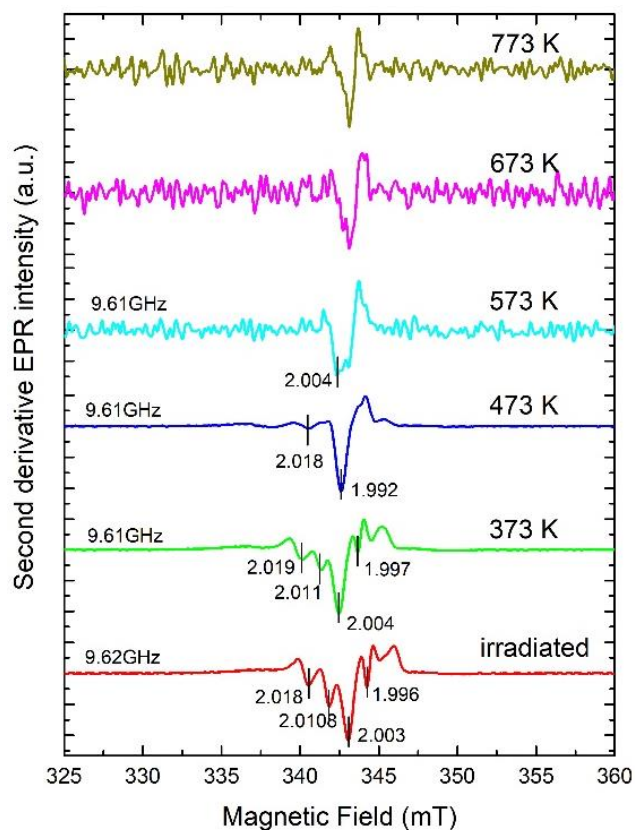


Table S8. The g-values and defect types for LiNaBSi glass irradiated with 5 MGy annealed for 24 hours at different temperatures.

LiNaBSi 5 MGy 16 hrs									
373 K		473 K		573 K		673 K		773 K	
g-value	defect	g-value	defect	g-value	defect	g-value	defect	g-value	defect
2.019	BOHC	2.018	POR	2.004	POR	Annihilated/Recombined			
2.011	BOHC	1.992	POR	low S/N	-				
2.004	BOHC	low S/N	-	low S/N	-				
1.997	ET	low S/N	-	low S/N	-				

Figure S18. Temperature vs log area for the integral of the first derivative EPR intensity of 0.5 MGy NaBaBSi glass.

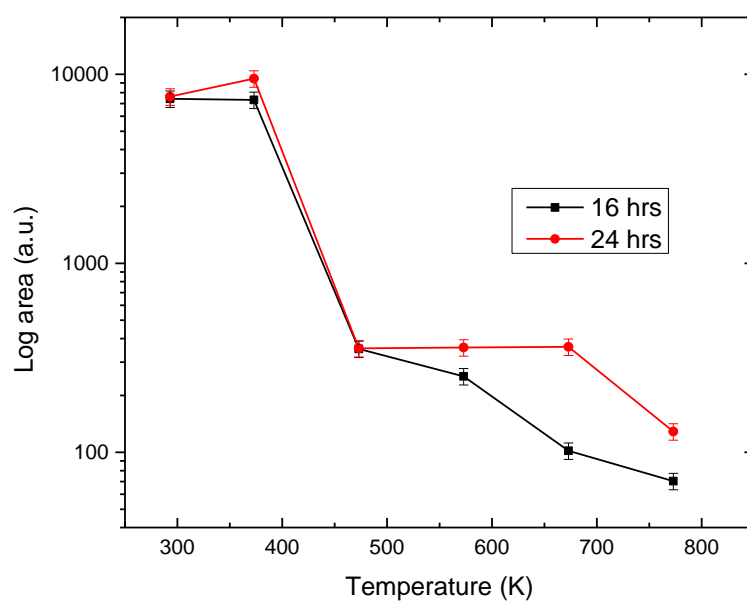


Figure S19. Temperature vs log area for the integral of the first derivative EPR intensity of 5 MGy NaBaBSi glass.

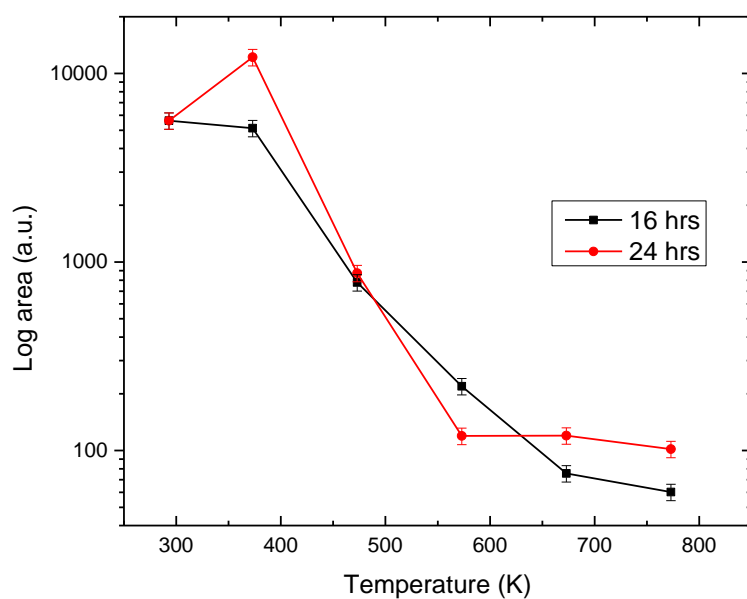


Figure S20. Temperature vs log area for the integral of the first derivative EPR intensity 0.5 MGy LiNaBSi glass.

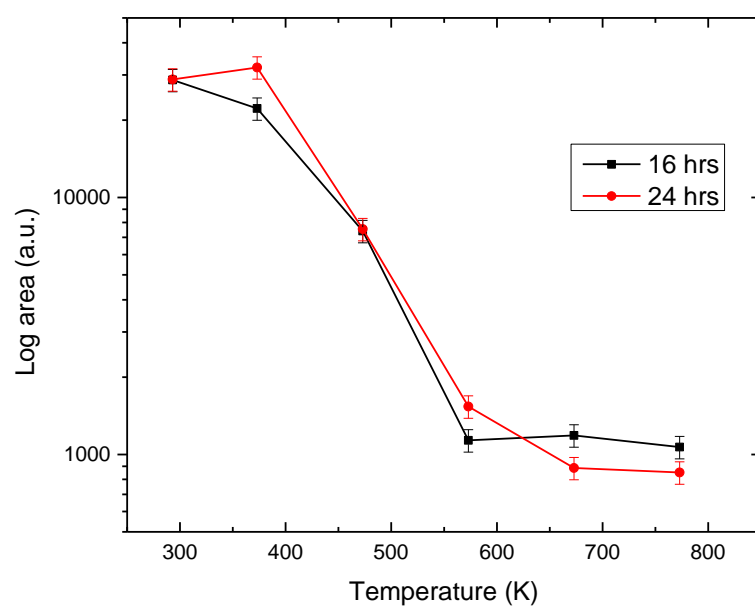


Figure S21. Temperature vs log area for the integral of the first derivative EPR intensity 5 MGy LiNaBSi glass.

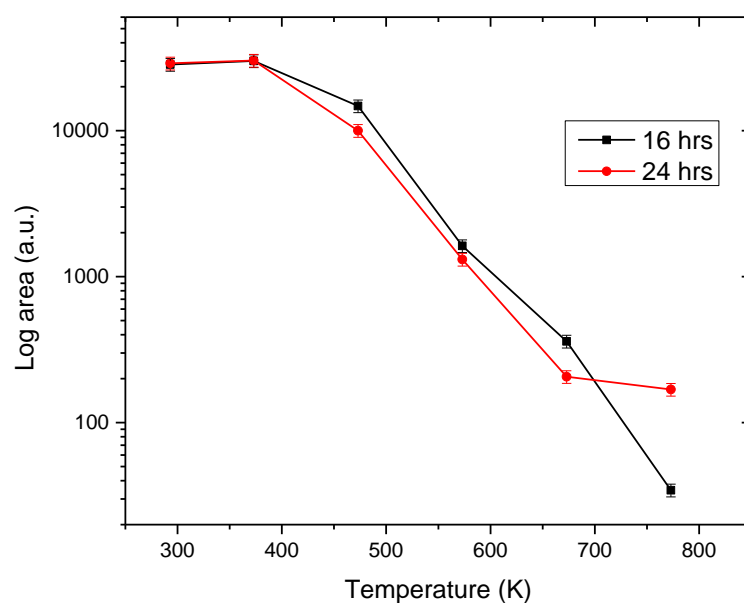


Figure S22. Tauc plot for optical band gap for (i) pristine, (ii) 0.5 and (iii) 5 MGy irradiated NaBaBSi glass specimens.

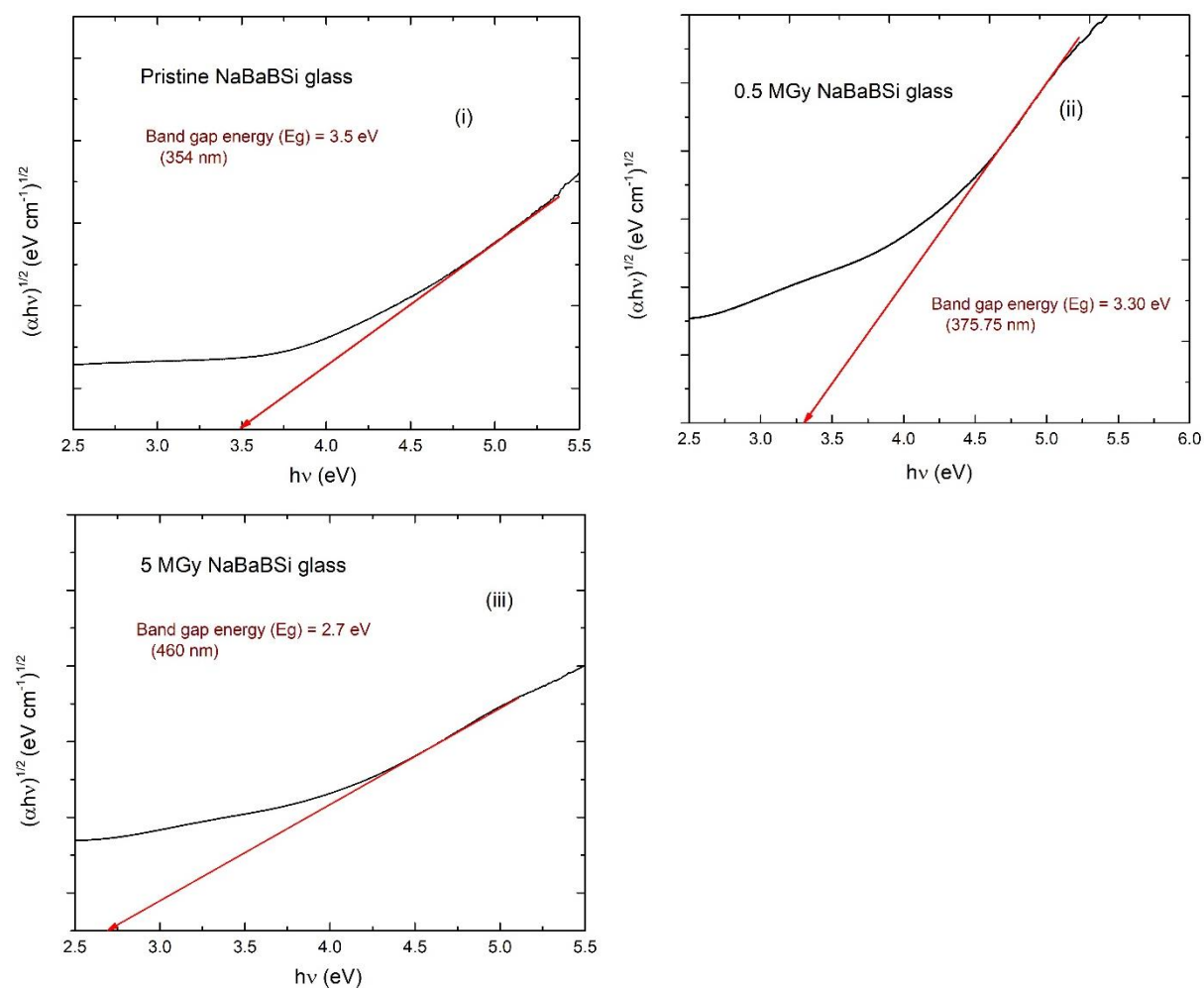


Figure S23. Tauc plot for optical band gap for (i) pristine (ii) 0.5 and (iii) 5 MGy irradiated LiBaBSi glass specimens.

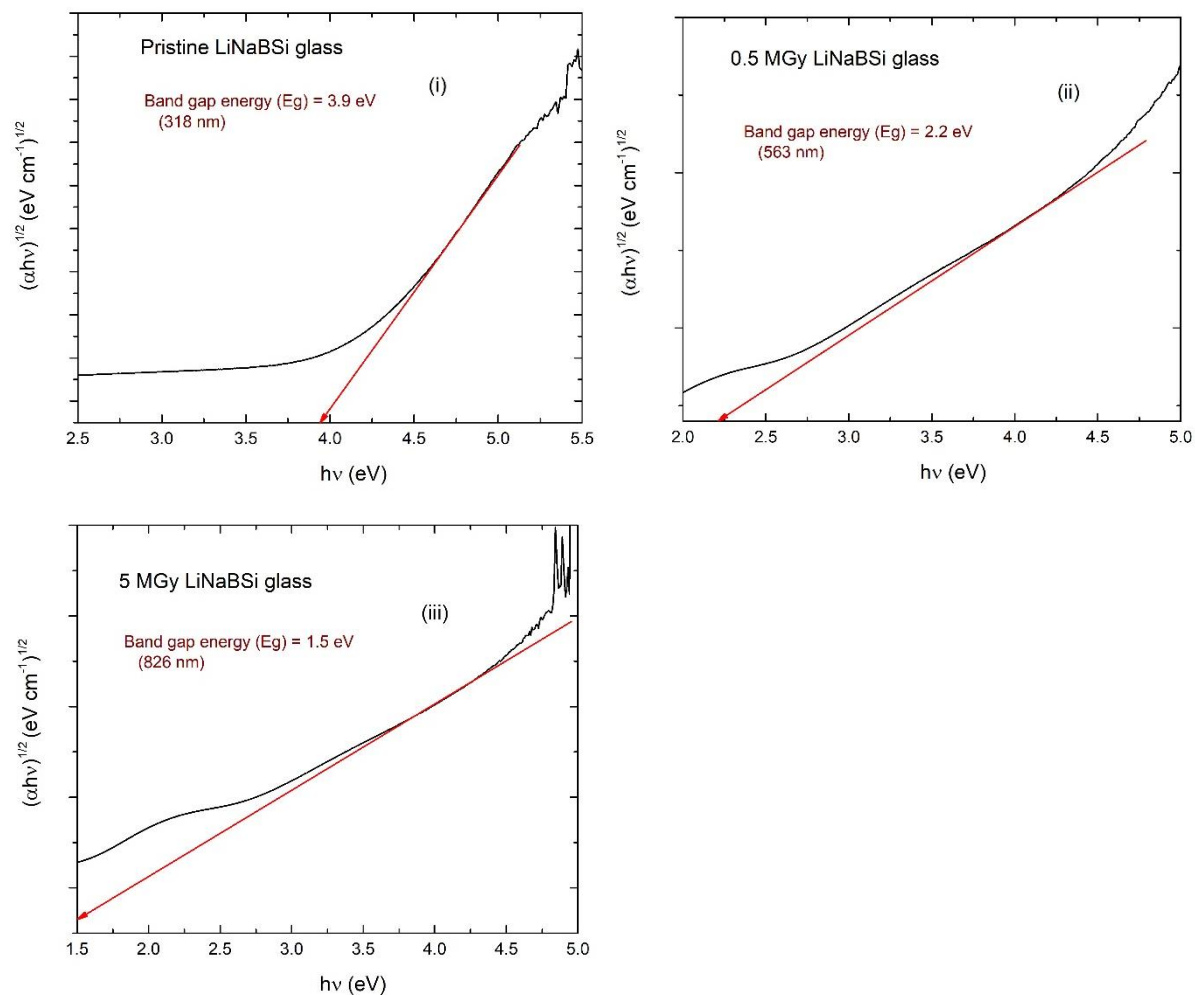


Table S9. Deconvolution and fitting parameters for UV-Vis-nIR spectra.

Parameter		LiNaBSi		NaBaBSi	
		0.5 MGy	5.0 MGy	0.5 MGy	5.0 MGy
Reduced χ^2		0.40202	0.24107	2.46828	4.50537
R^2		0.99629	0.9993	0.99962	0.99967
	ν_l	17620 cm^{-1}	16084 cm^{-1}	15636 cm^{-1}	15224 cm^{-1}
	λ_l	568 nm (BOHC + peroxy radicals)	622 nm (BOHC)	639 nm (E- centre + peroxy radicals)	657 nm (E- centre + peroxy radicals)
	A_l	341412 (7.69%)	64983 (0.86%)	81602 (10.27%)	62725 (4.27%)
	$\Delta\nu_l$	5936 cm^{-1}	4380 cm^{-1}	4945 cm^{-1}	4444 cm^{-1}

	ν_2	28274 cm ⁻¹	16161 cm ⁻¹	18969 cm ⁻¹	17618 cm ⁻¹
	λ_2	354 nm (BOHC)	551 nm (BOHC)	527 nm (BOHC)	568 nm (BOHC)
	A_2	2298160 (51.73%)	397338 (5.72%)	61154 (7.70%)	82003 (5.58%)
	$\Delta\nu_2$	12215 cm ⁻¹	6145 cm ⁻¹	7367 cm ⁻¹	5864 cm ⁻¹
	ν_3	34580 cm ⁻¹	26565 cm ⁻¹	30883 cm ⁻¹	31321 cm ⁻¹
	λ_3	289 nm (Trapped electrons)	376 nm (BOHC)	324 nm (E- centre)	319 nm (E- centre)
	A_3	1397460 (31.46%)	1701740 (22.58%)	432366 (54.44%)	795898 (54.19%)
	$\Delta\nu_3$	7861 cm ⁻¹	11194 cm ⁻¹	14823 cm ⁻¹	18375 cm ⁻¹
	ν_4	38002 cm ⁻¹	36465 cm ⁻¹	39388 cm ⁻¹	40230 cm ⁻¹
	λ_4	263 nm (Trace Fe impurity)	274 nm (Trapped electrons)	253 nm (Trace Fe impurity)	249 nm (Trace Fe impurity)
	A_4	405291 (9.12%)	5370910 (71.28%)	219076 (27.58%)	528043 (35.95%)
	$\Delta\nu_4$	4856 cm ⁻¹	5661 cm ⁻¹	6663 cm ⁻¹	8588 cm ⁻¹

Table S10. Summary of materials, methods, and results from literature in which formation of metallic colloid sodium is discussed, and in which other radiation induced optical absorption bands are reported.

Study	Material	Radiation type	Result	Analysis
Hassib <i>et al.</i> (1977) [85]	Sodalite	X-ray	Formation of colloidal aggregates (Na), blue coloration, EPR signal at 2.011	EPR, Optical transmission
Groote <i>et al.</i> (I) (1994) [86]	NaCl	Electron beam	F-defect centres T<65°C, Na colloids at higher T, absorption band b/w 550-600nm	Optical absorption spectroscopy
Groote <i>et al.</i> (II) (1994) [90]	NaCl	Electron beam	Na colloids of different shape and size	Optical absorption spectroscopy
Groote <i>et al.</i> (III) (1994) [89]	NaCl	Electron beam	Different melting T is linked with different size of Na colloid	Differential scanning calorimetry
Weselucha-Birczyńska <i>et al.</i> (2011) [92]	Single crystals of natural blue halite	N/A	Plasmon band at 629 for navy blue and 621 nm for blue samples	Optical absorption spectroscopy
Tsai <i>et al.</i> (2014) [93]	Silicate glass	Gamma	Absorption band in the range 360-540, HC1 and HC2 defect centre, EPR signal at 2.01	EPR, Optical transmission spectroscopy

Zatsepin <i>et al.</i> (2012) [37]	Sodium silicate glass	Gamma	HC1, HC2, and E ⁻ centre (g~1.97)	EPR
Mahadik <i>et al.</i> (2018) [95]	Natural halite	N/A	F-centres, Na colloids	Photoluminescence, Micro-Raman spectroscopy
Jiang <i>et al.</i> (2008) [94]	Sodium silicate glass	Electron beam	Formation of metallic sodium identified by plasmon at 5.8 eV	Electron energy loss spectroscopy
Manara <i>et al.</i> (1984) [96]	Borosilicate glass	Electron beam	Na moves towards the periphery, concentrated in a possible colloidal form	Energy dispersive X-ray analysis
Fayad <i>et al.</i> (2018) [68]	Borosilicate glass doped with yttrium oxide	Gamma	Absorption band at 229 nm related to Fe impurities and visible band b/w 500-600 due to BOHC or NBOHC	XRD, FTIR, optical absorption spectroscopy
El-Alaily <i>et al.</i> (2018) [71]	Barium borosilicate glass doped with titanium oxide	Gamma and heat treatment	Absorption band at 240 nm due to trace Fe impurity	SEM, Infrared, optical absorption, and transmission spectroscopy
Kolobkova <i>et al.</i> (2015) [87]	Sodium fluorophosphate glasses	Heat treatment	Surface plasmon b/w 400-450 nm	Heat treatment
Bochkareva <i>et al.</i> (2016) [88]	Na containing silicate glasses	Electron beam and subsequent heat treatment	Na nanoparticles characterised by plasmon resonance band at 405-410 nm	Optical absorption spectroscopy
Jiang <i>et al.</i> (2007) [69]	Na silicate glasses	Electron beam	Bulk plasmon band at 5.8 eV (214 nm) and surface plasmon at 3.9 eV (318 nm)	TEM and EELS
Griscom <i>et al.</i> (1998) [66]	Fused silica	Gamma	Combination of band due to peroxy-radicals and NBOHC at ~620 nm	Differential optical absorption spectroscopy
Bishay (1969) [73]	Alkali silicate glass	Gamma	Hole centre at 590-620, 427-450 nm	EPR, Optical absorption spectroscopy
Mackey <i>et al.</i> (1966) [67]	Sodium silicate glass	X-ray	Absorption band b/w 600-730 nm (E ⁻ centre), 326-413 nm due to trapped holes	Optical absorption spectroscopy
Mackey <i>et al.</i> (1966) [70]	Sodium disilicate glass doped with Eu ³⁺	X-ray	Absorption band 305 nm trapped electrons, 460 and 620 nm due to trapped holes	Optical absorption spectroscopy
